

# Entanglement Entropy and Twist Fields

*Michele Caraglio, Ferdinando Gliozzi*

Dipartimento di Fisica Teorica, Università di Torino and  
INFN, Sezione di Torino, via P. Giuria, 1, I-10125 Torino, Italy

## Abstract

The entanglement entropy of a subsystem  $A$  of a quantum system is expressed, in the replica approach, through analytic continuation with respect to  $n$  of the trace of the  $n$ -th power of the reduced density matrix. This trace can be thought of as the vacuum expectation value of a suitable observable in a system made with  $n$  independent copies of the original system. We use this property to numerically evaluate it in some two-dimensional critical systems, where it can be compared with the results of Calabrese and Cardy, who wrote the same quantity in terms of correlation functions of twist fields of a conformal field theory. Although the two calculations match perfectly even in finite systems when the system  $A$  consists of a single interval, they disagree whenever the subsystem  $A$  is composed of more than one connected part. The reasons of this disagreement are explained.

# 1 Introduction

In a quantum system, performing a local measurement may instantaneously affect local measurements far away. This is a manifestation of the quantum entanglement. A useful measure of this property in extended quantum systems with many degrees of freedom is the von Neumann or entanglement entropy: one considers a pure quantum state  $|\Psi\rangle$  (typically the ground state) that can be subdivided into two subsystems  $A$  and  $B$  and constructs the reduced density matrix

$$\rho_A = \text{tr}_B |\Psi\rangle\langle\Psi| \quad (1.1)$$

by tracing over the degrees of freedom of  $B$ . The von Neumann or entanglement entropy is defined to be

$$S_A \equiv -\text{tr} \rho_A \ln \rho_A = -\text{tr} \rho_B \ln \rho_B \equiv S_B . \quad (1.2)$$

Of particular interest is the case in which the two subsystems  $A$  and  $B$  correspond to two connected regions (the “outside” and the “inside”) in the space-time, where it was argued that the entanglement (or geometric) entropy is deeply related to the physics of the black holes[1, 2, 3]. An important element of the present understanding is its holographic interpretation [5]. This point of view seems to indicate a purely geometric way of computing the entanglement entropy in strongly coupled conformal field theories [6].

The entanglement entropy has been also extensively studied in low dimensional quantum systems as a new tool to investigate the nature of quantum criticality [7, 8, 9, 10, 11]. Several different calculations based on the conformal field theory (CFT) describing the universal properties of the quantum phase transition describing 1+1 dimensional systems, like quantum spin chains, have shown that the entropy grows logarithmically with the size  $\ell$  of the subsystem  $A$  as [7, 8, 9, 10]

$$S_A = \frac{c}{3} \ln(\ell/a) , \quad (1.3)$$

where  $c$  is the conformal anomaly and  $a$  an ultraviolet cutoff.

The trace of the  $n$ -th power of the reduced density matrix, which could be identified with the Tsallis entropy [12], plays a major role in the replica approach to entanglement entropy [10], yielding

$$S_A = -\lim_{n \rightarrow 1} \frac{\partial}{\partial n} \text{tr} \rho_A^n . \quad (1.4)$$

Our goal in this paper is to describe a simple method to directly measure  $\text{tr} \rho_A^n$  in whatever local lattice field theory in any space-time dimension, based on the observation that this quantity can be expressed, as we shall explain below, as the vacuum expectation value of

a suitable observable defined in a system made with  $n$  independent copies of the original quantum system.

We apply our method to check various consequences of the replica approach in some  $(1 + 1)$ -dimensional critical quantum system described by a relativistic conformal field theory (CFT), including a system with  $c < 0$ , where the entanglement entropy appears to be negative, finding also in that case complete agreement: evidently in those non-unitary systems the mixed state obtained by tracing over the degrees of freedom of  $B$  is more ordered than the pure state  $|\Psi\rangle$ .

When the subsystem  $A$  consists of  $N$  disjoint intervals  $A \equiv (u_1, v_1) \dots (u_N, v_N)$  the quantity  $\text{tr } \rho_A^n$  is proportional, at criticality, to the  $n$ -th power of the correlation function of  $2N$  local primary operators of complex scaling dimensions

$$\Delta_n = \bar{\Delta}_n = \frac{c}{24} \left(1 - \frac{1}{n^2}\right) \quad (1.5)$$

sitting on the end points of the  $N$  intervals:

$$\text{tr } \rho_A^n \propto \left\langle \prod_{j=1}^N \Phi_n^-(u_j, \bar{u}_j) \Phi_n^+(v_j, \bar{v}_j) \right\rangle^n. \quad (1.6)$$

Notice that these primary operators do not belong to the Kac table. They can be considered as a special kind of twist fields, called branch-point twist fields [13], because they are naturally related to the branch points in the  $n$ -sheeted Riemann surface where the system is defined in its Euclidean functional integral formulation. These primary operators also carry a conserved charge related to the orientation of the intervals.

The proof of the above statements relies (among other things) on the clever observation [10] that the vacuum expectation value of the stress tensor  $T(z)$  near a branch point has the same functional dependence as the one generated by a primary operator with scaling dimensions  $\Delta_n$ . Since the same branch point is present in each sheet of the Riemann surface, it is easy to conclude that  $\text{tr } \rho_A^n$  has the form (1.6).

By making a further assumption we shall discuss in the next Section, the authors of [10] proposed an explicit functional form <sup>1</sup>

$$\text{tr } \rho_A^n \propto \left| \frac{\prod_{j < k \leq N} (u_k - u_j)(v_k - v_j)}{\prod_{j, k \leq N} (v_k - u_j)} \right|^{4n\Delta_n}, \quad (1.7)$$

---

<sup>1</sup>There is a typo in this formula in [10]. We thank P.Calabrese for pointing this out to us.

Note that the points of type  $u$  and of type  $v$ , associated respectively with  $\Phi_n^-$  and  $\Phi_n^+$ , are treated in a different way. This is justified only when the intervals are intrinsically oriented, which is not the case when  $n = 2$ , where all the branch points are on the same footing and  $\Phi_2^-(w) \equiv \Phi_2^+(w)$ . We shall discuss below the  $N = n = 2$  case in detail. When  $n$  is an odd number and  $c > 0$  we shall argue, and corroborate with numerical experiments, that whenever two twist fields of the same charge approach each other the above quantity develops an ultraviolet divergence instead of vanishing as (1.7) would require.

The origin of such a discrepancy can be traced to the assumption that the only singularities of  $T(z)$  are the double poles at the branch points of the multi-sheeted Riemann surface, which is not the case of the conformal mappings  $w = f(z)$  considered in [10]. This point will be further discussed in the next Section.

The contents of this paper are as follows. In the next Section we summarise the main results of the replica approach to entanglement entropy in CFT and discuss some difficulties in the use of the conformal mappings when the number of branch points is larger than two. In the following Section we describe our method of evaluating  $\text{tr} \rho_A^n$  as the vacuum expectation value of a suitable observable; as a byproduct we uncover a special quantum symmetry, which is exact only at zero temperature, yielding at once the important identity  $\text{tr} \rho_A^n = \text{tr} \rho_B^n$  and other useful relationships. In Section 4 we implement the method in some specific two-dimensional systems, namely the Potts models: they can be easily simulated at their critical point and the corresponding CFT is known. We finish with some conclusions.

## 2 Conformal maps and twist fields

Translational and rotational invariance of a CFT on the complex  $z$ -plane  $\mathbb{C}$  imply  $\langle T(z) \rangle_{\mathbb{C}} = 0$ . Under a conformal mapping  $w \rightarrow z = f(w)$  the stress tensor  $T$  transforms as

$$T(w) = \left( \frac{df}{dw} \right)^2 T(z) + \frac{c}{12} \{f, w\} \quad (2.1)$$

where

$$\{f, w\} = \frac{f'''}{f'} - \frac{3}{2} \left( \frac{f''}{f'} \right)^2 \quad (2.2)$$

is called Schwarzian derivative. Comparing the vacuum expectation value of both sides of (2.1) yields

$$\langle T(w) \rangle_{\mathcal{R}} = \frac{c}{12} \{f, w\} \quad (2.3)$$

where  $\mathcal{R}$  is the Riemann surface associated with  $f(w)$ .

The identity  $\{f, w\} = -2\sqrt{f'} \frac{d^2}{dw^2} \frac{1}{\sqrt{f'}}$  implies at once that  $\{f, w\} \equiv 0$  if and only if  $f(w)$  is a linear fractional transformation, which is the only conformal mapping of the whole  $\mathbb{C}$  onto itself. In any other case  $\langle T(w) \rangle \neq 0$  and some symmetry of the original system is lost. In particular, using again the above-mentioned identity, it is easy to see that the only conformal mappings conserving translational invariance ( hence  $\langle T(w) \rangle_{\mathcal{R}} = \text{const.}$ ) are the exponential mappings, which can be written in a suitable basis in the form

$$z = \exp(2\pi \frac{w}{L}) , \quad (2.4)$$

which maps the cylinder composed of the infinite strip  $0 \leq \Im w \equiv y < L$  with periodic boundary conditions into the whole  $z$  plane excepted the origin. As a parenthetic remark, we note that this exponential mapping is the key ingredient to find universal finite size effects of two-dimensional field theories at criticality [14]. In any other conformal mapping, being  $\langle T(w) \rangle$  a non-constant analytic function, it has to be singular somewhere. By dimensional reasons, the isolated singularities of  $\langle T(w) \rangle$  are double poles.

As a simple illustrative example, apply (2.3) to the mapping  $z = f(w) = w^{\frac{1}{n}}$ . It yields at once

$$\langle T(w) \rangle_{\mathcal{R}_n} = \frac{c}{24} \frac{(1 - 1/n^2)}{w^2} , \quad (2.5)$$

where  $\mathcal{R}_n$  is now a  $n$ -sheeted Riemann surface branched over 0 and  $\infty$ . We can now first displace these points with a linear fractional transformation  $g(w) = \frac{w-u}{w-v}$  and then consider the composed transformation

$$z(w) = f(g(w)) = \left( \frac{w-u}{w-v} \right)^{\frac{1}{n}} . \quad (2.6)$$

Being  $g$  a linear fractional transformation, we may take advantage of the remarkable identity  $\{f(g), w\} = g'^2 \{f, g\}$  to get

$$\langle T(w) \rangle_{\mathcal{R}_n} = c \frac{(1 - 1/n^2)}{24} \frac{(u-v)^2}{(w-u)^2(w-v)^2} . \quad (2.7)$$

As first pointed out in [10], this expression coincides, up to a normalising constant, with the three-point function  $\langle T(w) \Phi_n(u, \bar{u}) \Phi_n(v, \bar{v}) \rangle_{\mathbb{C}}$  where  $\Phi_n(w, \bar{w})$  is a primary operator, called branch-point twist field [13], with complex scaling dimensions  $\Delta_n = \bar{\Delta}_n = c \frac{1-1/n^2}{24}$  associated with the branch points  $w = u$  and  $w = v$  of  $\mathcal{R}_n$ , as already anticipated in the Introduction. Combining such an observation with the fact that the surface constructed with the replica method has the same intrinsic geometric properties as  $\mathcal{R}_n$  Calabrese and Cardy

[10] were able to argue that

$$\mathrm{tr} \rho_A^n \propto \langle \Phi_n^-(u, \bar{u}) \Phi_n^+(v, \bar{v}) \rangle_{\mathbb{C}}^n = c_n \left| \frac{a}{u-v} \right|^{\frac{c}{6}(n-1/n)}, \quad (2.8)$$

where  $a$  is an UV cutoff and  $A$  is the interval joining the branch points  $u$  and  $v$ .

To make contact with numerical simulations it is useful to rewrite this correlator in a finite geometry using the transformation law of the primary operators under a suitable conformal mapping  $w = h(\zeta)$  :

$$\langle \Phi_n^-(\zeta_1, \bar{\zeta}_1) \Phi_n^+(\zeta_2, \bar{\zeta}_2) \rangle_{\mathcal{R}} = |w'(\zeta_1) w'(\zeta_2)|^{2\Delta_n} \langle \Phi_n^-(u, \bar{u}) \Phi_n^+(v, \bar{v}) \rangle_{\mathbb{C}}, \quad (2.9)$$

where  $\zeta_1$  and  $\zeta_2$  are the inverse images of  $u$  and  $v$  and  $\mathcal{R}$  is the Riemann surface associated with  $h$ . Using the exponential mapping (2.4) and arranging for instance the branch points to lie on the imaginary axis of the cylinder  $\zeta = x + iy$ , one finally finds [10]

$$\mathrm{tr} \rho_A^n = c_n \langle \Phi_n^-(y_1) \Phi_n^+(y_2) \rangle_{\mathrm{cyl.}}^n = c_n \left( \frac{\pi/L}{\sin(\pi\ell/L)} \right)^{\frac{c}{6}(n-1/n)}, \quad (2.10)$$

with  $\ell = |y_2 - y_1|$ .

We checked this formula with numerical experiments in two different critical systems, one, the Ising model, with positive conformal anomaly ( $c = \frac{1}{2}$ ) and the other, a  $Q$ -state Potts model with  $Q < 1$ , corresponding to a conformal theory with a negative conformal anomaly ( $c = -\frac{11}{14}$ ). In either case we studied the dependence on  $n$ ,  $L$  and  $\ell$ , finding perfect agreement with (2.10) provided the distances of the branch points and the sizes of the lattice are large enough with respect to the lattice spacing (see Section 4 for more details).

## 2.1 General case

When  $A$  consists of more than one disjoint interval, i.e.  $A \equiv (u_1, v_1) \dots (u_N, v_N)$ , it is natural to assume that the Tsallis entropy  $\mathrm{tr} \rho_A^n$  be proportional to the  $n$ -th power of the correlation function of the twist fields associated with the  $2N$  branch points (see Eq.(1.6)).

The Ward identities of the conformal invariance tell us that the only singularities of  $\langle T(w) \Phi_n^-(u_1, \bar{u}_1) \dots \Phi_n^+(v_N, \bar{v}_N) \rangle$  are the double poles located at  $u_j, v_j$  ( $j = 1 \dots N$ ). Calabrese and Cardy proposed the Ansatz

$$\frac{\langle T(w) \Phi_n^-(u_1, \bar{u}_1) \dots \Phi_n^+(v_N, \bar{v}_N) \rangle_{\mathbb{C}}}{\langle \Phi_n^-(u_1, \bar{u}_1) \dots \Phi_n^+(v_N, \bar{v}_N) \rangle_{\mathbb{C}}} \equiv \langle T(w) \rangle_{\mathcal{R}_{nN}} = \frac{c}{24} \{f_{nN}, w\}, \quad (2.11)$$

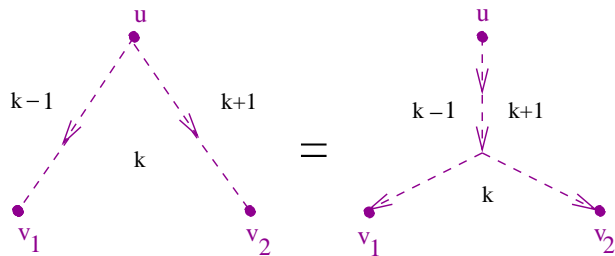


Figure 1: Three branch points generated by the fusion of two oriented intervals  $(u_1, v_1)(u_2, v_2)$  in the limit  $|u_1 - u_2| \rightarrow 0$ . A general symmetry of the replica approach described in Section 3.1 allows to deform the intervals as indicated on the right.

with

$$z = f_{nN}(w) = \prod_{j=1}^N \left( \frac{w - u_j}{w - v_j} \right)^{\frac{1}{n}} ; \quad u_j \neq u_k, \quad v_j \neq v_k \quad \forall j \neq k . \quad (2.12)$$

The condition  $u_j \neq u_k, v_j \neq v_k \quad \forall j \neq k$ , which is an important ingredient to derive (1.7), has no justification in the process of sewing the  $n$  replicas, as there is no geometrical obstruction in letting two branch points of the same type, say  $u$ , coincide, like in Figure 1.

The equality illustrated in Figure 1 comes from the fact that, in the physical systems we are studying, a cut joining two branch points may be continuously deformed, as we shall discuss in detail in the next Section. Note that the cut associated with the fused branch point sews together the sheets in the order  $k \rightarrow k + 2$ . Clearly the order in which the replicas are sewn together is immaterial, provided that all the  $n$  replicas are cyclically connected. On the other hand, if  $n$  is an odd number, the permutation  $k \rightarrow k + 2$  covers once all the  $n$  replicas. Therefore, according to the general argument of [10], the complex scaling dimensions of the twist field  $\Phi_n^{+2}$  arising from the fusion of two twist fields with equal charge are expected to be exactly the same, i.e.  $\Delta_n = \bar{\Delta}_n = \frac{c}{24}(1 - \frac{1}{n^2})$ . We can take advantage of this remarkable property to write down the operator product expansion (OPE)

$$\Phi_n^+(0, 0) \Phi_n^+(w, \bar{w}) = \frac{1}{|w|^{2\Delta_n}} \Phi_n^{+2}(0, 0) + \dots \quad (2.13)$$

where  $n$  is an odd number. The dots indicate less singular terms.

Similarly (2.8) yields

$$\Phi_n^+(0, 0) \Phi_n^-(w, \bar{w}) = \frac{c_n}{|w|^{4\Delta_n}} + \dots \quad (2.14)$$

Comparing (2.13) and (2.14) shows that two branch points of the same type develop, as the interdistance decreases, an UV singularity with an exponent which is exactly half the

exponent associated with a pair of branch points of opposite type, while (1.7) would predict a zero. A numerical check of this behaviour is illustrated in Figure 10.

In the limit configuration depicted in Figure 1,  $\text{tr } \rho_A^n$  becomes of course proportional to the  $n$ -th power of the three-point function

$$\text{tr } \rho^n(u, v_1, v_2) \propto \langle \Phi_n^{-2}(u, \bar{u}), \Phi_n^+(v_1, \bar{v}_1), \Phi_n^+(v_2, \bar{v}_2) \rangle_{\mathbb{C}}^n, \quad (2.15)$$

therefore conformal invariance completely fixes its functional dependence:

$$\text{tr } \rho^n(u, v_1, v_2) \propto \frac{1}{|(v_1 - v_2)(v_2 - u)(u - v_1)|^{2n\Delta_n}}, \quad (2.16)$$

which is valid for any odd  $n$ . A numerical check of the scaling behaviour of this quantity for  $n = 3$  can be found in Figure 9.

Going back to (2.11) and (2.12), note that they are based on two distinct assumptions:

- i)*  $\langle T(w) \rangle_{R_{nN}}$  can be written as the Schwarzian derivative of a suitable function  $f_{nN}$ ;
- ii)* this function is given by (2.12).

It is easy to prove that the latter assumption is not correct in the case of multi-intervals because the function  $f_{n,N>1}(w)$  does not fulfil the condition that the only singularities of its Schwarzian derivative  $\{f_{n,N}, w\}$  are the double poles at  $u_j$  and  $v_j$ , as conformal Ward identities require. A simple way to see it, is to put  $n = 1$  in (2.12), thereby eliminating all the branch points and the associated twist fields. If the only singularities of (2.11) were the double poles at  $u_j, v_j$  ( $j = 1 \dots N$ ) one should have  $\{f_{1N}, w\} = 0$ . This would imply, as emphasised at the beginning of this Section,  $f_{1N}(w)$  to be a linear fractional transformation, which evidently is not the case when  $N > 1$ . Actually we find, in the  $N = 2$  case,

$$\{f_{12}, w\} = -\frac{3}{2} \frac{1}{(w - r_1)^2} - \frac{3}{2} \frac{1}{(w - r_2)^2} + \frac{3}{r_1 - r_2} \left( \frac{1}{w - r_1} - \frac{1}{w - r_2} \right), \quad (2.17)$$

where  $r_1$  and  $r_2$  are the two roots of the equation  $\frac{df_{12}}{dw} = 0$ , namely

$$r_{1,2} = \frac{v_1 v_2 - u_1 u_2 \pm \sqrt{(u_1 - v_1)(v_1 - u_2)(u_2 - v_2)(v_2 - u_1)}}{u_1 - v_1 + u_2 - v_2}. \quad (2.18)$$

Since  $f_{n2} = (f_{12})^{1/n}$ , it is easy to verify that these double poles at  $r_i$  are present, with the same coefficient, for any value of  $n$ . Therefore the regular zeros of  $f'_{n2}$ , where the mapping  $w \rightarrow f_{n2}$  is not invertible, behave like (fake) primary operators of complex scaling dimensions



$\delta_n = \bar{\delta}_n = -\frac{c}{16}$ . Hence  $\{f_{n,2}, w\}$  has unwanted singularities besides those associated to the branch points.

On the contrary, in the case of a single interval it is straightforward to write down the inverse function  $w(z) = f_{n,1}^{-1}(z)$  which solves the ordinary differential equation (ODE)

$$w'^n \propto (w-u)^{n-1}(w-v)^{n+1} \quad , \quad (2.19)$$

showing that the only points where this conformal mapping is not invertible are just the branch points  $u$  and  $v$ .

Having proved that when  $N > 1$  (2.12) is not a solution of (2.11), the question arises as to whether there is any solution of such an equation. A crucial observation is that the  $n$ -sheeted Riemann surface  $\mathcal{R}_{n,N}$  with  $N > 1$  is topologically inequivalent to the complex plane  $\mathbb{C}$ . *A fortiori* there is no way to conformally map  $\mathcal{R}_{n,N>1}$  onto  $\mathbb{C}$ . As a consequence, one cannot longer use the main physical motivation outlined at the beginning of this Section, namely that the vanishing of  $\langle T \rangle_{\mathbb{C}}$  leads to express  $\langle T(w) \rangle_{\mathcal{R}_{n,N>1}}$  as a Schwarzian derivative. However this argument does not exclude *a priori* that  $\langle T(w) \rangle_{\mathcal{R}_{n,N>1}}$  is a Schwarzian derivative for some other reason. Thus we can try to find possible solutions of (2.11).

From a mathematical point of view the problem can be reformulated as follows: find a function  $z(w)$  such that *i*) its Schwarzian derivative  $\{z, w\}$  is singular only at the branch points  $u_1, u_2, \dots, u_{2N}$  of  $R_{n,N}$ ; *ii*) these singularities are double poles; *iii*) the coefficient<sup>2</sup> of  $(w-u_i)^{-2}$  is  $\frac{1-1/n^2}{2}$ . We shall see that this problem admits very few solutions which can be explicitly constructed.

As a starting point of this analysis, notice that it is always possible to map a connected domain of  $\mathbb{C}$  (with some boundary identified) onto  $R_{n,N}$ . For instance  $\mathcal{R}_{2,2}$ , the double cover of the plane  $w$  branched over  $u_1, u_2, u_3, u_4$ , is conformally equivalent to a torus, represented by a parallelogram  $\mathcal{D}$  of the  $z$ -plane with opposite sides identified. The ODE (2.19) is now replaced by

$$w'^2 \propto (w-u_1)(w-u_2)(w-u_3)(w-u_4) \quad . \quad (2.20)$$

Its general solution may be brought into the form

$$w(z) \propto \frac{1}{\wp(z)} + u_1 \quad , \quad (2.21)$$

where  $\wp(z)$  is the elliptic  $\wp$ -function of Weierstrass associated with the mentioned parallelogram. Since the singularities of  $\{z, w\}$  coincide with the zeros of  $w'$  the first condition is

---

<sup>2</sup> The last condition implies that the scaling dimension of the associated primary field is  $\Delta_n$ .

fulfilled. An explicit, straightforward, calculation yields

$$\{z, w\} = \sum_{i=1}^4 \left[ \frac{3}{8} \frac{1}{(w - u_i)^2} - \frac{1}{4} \frac{1}{w - u_i} \sum_{j \neq i} \frac{1}{u_i - u_j} \right], \quad (2.22)$$

which is the sought after behaviour. It shows, once again, that in the  $\mathcal{R}_{2,2}$  case the solution of (2.11) is not (2.12), but the inverse of the function (2.21)<sup>3</sup>.

One may envisage a straightforward extension of (2.19) and (2.20) by looking for solutions of the equation

$$w'^n \propto P(w), \quad (2.23)$$

where  $P(w)$  is zero or singular only on the branch points  $u_j, v_j$  ( $j = 1, \dots, N$ ). It may be worth observing that evaluating  $\{z, w\}$  does not require the actual knowledge of the solution of (2.23): using the identity  $\{z, w\} = -\{w, z\}/w'^2$  we obtain

$$\{z, w\} = \frac{(2n - 1) \dot{P}^2 - 2n \ddot{P} P}{2n^2 P^2}, \quad (2.24)$$

where  $\dot{P} = \frac{dP}{dw}$  and  $\ddot{P} = \frac{d^2P}{dw^2}$ .

Contrarily to naive expectations, there are very strong restrictions on the possible form of  $P(w)$  if we are to exclude branch points associated to primary fields with negative scaling dimensions. First,  $P(w)$  must be a polynomial of degree  $2n$  at most. However, if the degree is less than  $2n$  there is a branch point at infinity on the  $n$ -sheeted Riemann surface, thus we assume that  $P(w)$  is exactly of degree  $2n$  in  $w$ , but this is not yet sufficient. It is worth noting that the absence of negative scaling dimensions coincide with the requirement that there are no movable singularities [15], i.e. singularities of the solution  $w(z)$  which move in the  $z$ -plane as the initial values are varied.

If we demand either the absence of movable singularities or the positivity of the scaling dimensions of the involved twist fields, it turns out that there are essentially only six types of allowed ODE of the kind (2.23)<sup>4</sup>. Two of them are (2.19) and (2.20). A third type is simply a limit case of (2.20) when  $u_1 = u_2$ . The other three types are

$$w'^3 \propto (w - u_1)^2(w - u_2)^2(w - u_3)^2, \quad (2.25)$$

$$w'^4 \propto (w - u_1)^3(w - u_2)^3(w - u_3)^2, \quad (2.26)$$

$$w'^6 \propto (w - u_1)^5(w - u_2)^4(w - u_3)^3. \quad (2.27)$$

---

<sup>3</sup>This inverse function may be expressed in terms of an elliptic integral of the first kind.

<sup>4</sup>See for instance [15], p.312ff.

They describe multi-sheeted Riemann surfaces branched over three points as depicted in Figure 1. In particular the first, once inserted in (2.24) and combined with the conformal Ward identities, leads to (2.16) with  $n = 3$ . The latter two correspond to  $n = 4$  and  $n = 6$  and could therefore be used for hints to extend the OPE (2.13) to even  $n$ .

Comparison of (2.22) with the conformal Ward identity associated to  $\langle T(w) \rangle_{\mathcal{R}_{2,2}}$  suggests

$$\text{tr } \rho^2(u_1, u_2, u_3, u_4) \propto \prod_{j < k \leq 4} \frac{1}{|u_j - u_k|^{c/12}} . \quad (2.28)$$

This expression has the expected symmetry properties under the permutations of the branch points; note also that rescaling all the coordinates by a common scale factor  $u_i \rightarrow \lambda u_i$  yields  $\text{tr } \rho^2(\lambda u_i) = \lambda^{-c/2} \rho^2(u_i)$ , which is the expected scaling property of the square correlator of four twist fields (see also (4.5)). However Eq. (2.28) cannot be trusted because it implies, as it would be simple to show, the unwanted identity  $\langle T(z) \rangle_{\mathcal{D}} \equiv 0$ , where  $\mathcal{D}$  is the parallelogram of the  $z$ -plane conformally equivalent to  $\mathcal{R}_{2,2}$ .

Summing up, we have shown that Eq. (2.11) has no other solutions besides the two-point and some three-point correlation functions. Thus the problem of finding the entanglement entropy of disjoint intervals remains open.

### 3 $\text{tr } \rho_A^n$ as a vacuum expectation value

In this section we explicitly write  $\text{tr } \rho_A^n$  in whatever quantum system as the vacuum expectation value of a suitable observable  $\mathbb{O}$ , defined on a larger system composed of  $n$  decoupled copies of the original system. This method is particularly well suited for numerical simulations because a single numerical experiment directly yields the value of  $\text{tr } \rho_A^n$ .

The partition function  $Z = \text{tr } e^{-\beta H}$  of our  $d$ -dimensional quantum system at inverse temperature  $\beta$  can be computed in a standard way by doing the Euclidean functional integral in a  $d + 1$ -dimensional hyper-cubic lattice  $\Lambda = \{\vec{x}, \tau\}$  ( $x_i, \tau \in \mathbb{Z}$ ) over fields  $\phi(x) \equiv \phi(\vec{x}, \tau)$  periodic under  $\tau \rightarrow \tau + \beta$ . Therefore the system composed of  $n$  independent replicas of the original system is described by the  $n$ -th power of  $Z$ :

$$Z^n = \int \prod_{k=1}^n \mathcal{D}[\phi_k] e^{-\sum_{k=1}^n S[\phi_k]} , \quad (3.1)$$

where  $\phi_k$  is a field configuration associated with the  $k$ -th replica and  $S[\phi]$  is the Euclidean action. Though the method has a much wider applicability, we assume, for the sake of

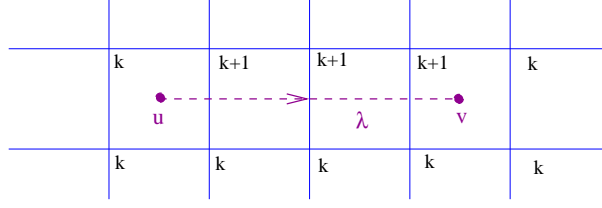


Figure 2: The branch points in a square lattice are located on the sites of the dual lattice. The links intersecting the cut  $\lambda$  connect two consecutive planar lattices labelled by  $k$  and  $k + 1 \pmod{n}$ .

simplicity, that the fields  $\phi_k$  are associated with the nodes of the lattice and that  $S$  is the sum of contributions of the nodes and the links of the lattice  $\Lambda$

$$S[\phi_k] = \sum_{x \in \Lambda} V(\phi_k(x)) + \sum_{\langle xy \rangle} F(\phi_k(x), \phi_k(y)) , \quad (3.2)$$

with  $\langle xy \rangle$  ranging over pairs of adjacent nodes in  $\Lambda$ ;  $V$  and  $F$  are arbitrary functions.

To define the coupled action  $S_A^{(n)}[\phi_1, \phi_2, \dots, \phi_n]$ , let us begin with a two-dimensional system defined in a square lattice. The subsystem  $A$  consists of one (or more) segments joining pairs of nodes in the dual lattice  $\tilde{\Lambda}$ . We now connect these pairs of nodes with a line  $\lambda$ , not necessarily coinciding with the segments of  $A$ , and replace each link intersecting this line with a link connecting two consecutive sheets,  $k$  and  $k + 1$ , in a cyclical order (see Figure 2). In this way we obtain a discretized version of a  $n$ -sheeted Riemann surface where the two points on the dual lattice are the branch points and the line  $\lambda$  is the cut. The associated coupled action is

$$S_A^{(n)} = \sum_{k=1}^n \left[ \sum_{x \in \Lambda} V(\phi_k) + \sum_{\langle xy \rangle \notin \lambda} F(\phi_k(x), \phi_k(y)) + \sum_{\langle xy \rangle \in \lambda} F(\phi_k(x), \phi_{k+1 \pmod{n}}(y)) \right] . \quad (3.3)$$

The generalisation to higher dimensions is almost obvious: in a  $2 + 1$  dimensional system the two (or more) branch points are replaced by one (or more) closed paths  $\gamma$  on the dual lattice and  $\lambda$  is replaced by a surface  $\Sigma$  whose boundary is  $\gamma$ , and so on.

The observable we are interested in is

$$\mathbb{O} = e^{-\left(S_A^{(n)}[\phi_1, \phi_2, \dots, \phi_n] - \sum_{k=1}^n S[\phi_k]\right)} . \quad (3.4)$$

Its vacuum expectation value in the system of  $n$  independent copies of the original system is

$$\langle \mathbb{O} \rangle_n = \frac{\int \prod_{k=1}^n \mathcal{D}\phi_k \mathbb{O} e^{-S[\phi_k]}}{Z^n} = \frac{\int \prod_{k=1}^n \mathcal{D}\phi_k e^{-S_A^{(n)}}}{Z^n} = \frac{Z_n(A)}{Z^n} = \text{tr } \rho_A^n . \quad (3.5)$$

$Z_n(A)$  is the partition function of the system in the  $n$ -sheeted Riemann surface or of its multi-dimensional generalisations. The reduced density matrix  $\rho_A$  is normalised as in [10].

In numerical simulations this observable can be evaluated with great accuracy, because only the links intersecting the cut  $\lambda$  (or its multi-dimensional generalisation) contribute to it. Actually, it is not necessary to simulate  $n$  independent systems: simulating a single system and taking, for each measurement of  $\mathbb{O}$ ,  $n$  statistically independent configurations is enough. Alternatively, as a consistency check of the algorithm, one may simulate the system on a  $n$ -sheeted Riemann surface (or its multi-dimensional generalisations) and verify that in such a case one should obtain

$$\langle \mathbb{O}^{-1} \rangle_{\mathcal{R}} = \frac{Z^n}{Z_n(A)}. \quad (3.6)$$

### 3.1 A useful symmetry

A system composed of  $n$  decoupled copies of the same  $d$ -dimensional quantum system has an interesting invariance which is something more than the standard replica symmetry considered in disordered systems. Let us assume that the system in its Euclidean description is defined on a stack  $\{\Lambda_k, k = 1, \dots, n\}$  of  $n$  copies of a  $d+1$  dimensional hyper-cubic lattice. Each node of the stack is characterised by  $d+2$  integral coordinates  $(x_1, x_2, \dots, x_{d+1}, k)$  with  $1 \leq k \leq n$ . Assume furthermore an imaginary time coordinate  $x_{d+1}$  running from  $-\infty$  to  $\infty$  (i.e. zero temperature) and define the following transformation

$$x_i \rightarrow x_i \quad (i = 1, 2, \dots, d+1) \quad ; \quad k \rightarrow \begin{cases} k & \text{if } x_{d+1} \leq \alpha \\ k - 1 \pmod{n} & \text{if } x_{d+1} > \alpha \end{cases} \quad (3.7)$$

where  $\alpha$  is an arbitrary real number. This transformation may be thought of as a simple relabelling of nodes of the stack: after such a transformation the system consists always of  $n$  disjoint lattices, with exactly the same geometric structure as before the transformation; the only difference is that the label  $k$  is no longer constant along a given copy. As a consequence, the partition function  $Z^n$  of the composed system is obviously invariant under such a transformation. Note however that it is not a symmetry of the classical action  $\sum_k S[\phi_k]$ : one has to perform the functional integration in order to implement this invariance; therefore in a sense it can be considered to be a quantum symmetry. The above considerations can be generalised in an obvious way to the coupled system described by the partition function  $Z_n(A)$ .

To make the discussion concrete and explicit, we specialise to the case where the field theory in question is defined on an infinite cylinder of circumference  $L$  (see Figure 3). The

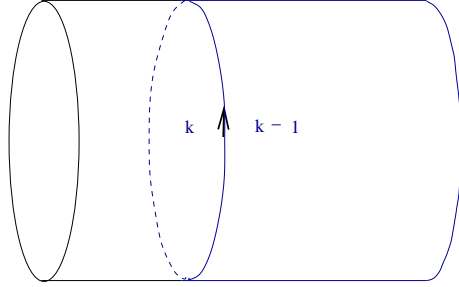


Figure 3: The  $k$  labels of the nodes of the stack of  $n$  cylinders after the transformation (3.7).

transformation just defined could be also generated by the  $n$ -sheeted Riemann surface described in Figure 2 by moving the two end points in opposite directions in such a way that the cut  $\lambda$  does wrap around the cylinder. In the limit where the end points touch each other, they annihilate and disappear, and the  $n$ -sheeted Riemann surface becomes a stack of  $n$  disjoint cylinders. Thus, the symmetry generated by the transformation (3.7) can be viewed as the invariance of the system under the addition (or the removal) of closed cuts wrapped around the cylinder. We can enlarge the game by also considering cuts associated with homotopically trivial loops, which can be used for instance to show that the cut  $\lambda$  connecting two branch points may undergo continuous deformations, or to prove identities of the kind

$$\mathrm{tr} \rho_{A=\{(u_i, v_i) (u_j, v_j) \dots\}}^n \equiv \mathrm{tr} \rho_{A=\{(u_i, v_j) (u_j, v_i) \dots\}}^n . \quad (3.8)$$

This point is illustrated in Figure 4. In words, these identities show that the cuts or intervals associated with the branch points  $u_j$  and  $v_j$  are in no way distinguished lines on the surface: their introduction has a similar role as the choice of a reference frame on the surface. Note that the essential physics responsible for this symmetry is not some special effect of CFT, but rather a general property of the functional integration - a basic tenet of generic quantum field theories.

If we combined together open and closed cuts associated with arbitrary permutations of replicas, a very rich structure would emerge. However it goes beyond the scope of this paper. In the following, we consider for convenience only cyclical or anti-cyclical permutations of the replicas.

Two points  $u$  and  $v$  on a cylinder can be connected by a cut  $\lambda$  in two topologically inequivalent ways (see Figure 5). These two ways correspond to the two complementary subsystems  $A$  and  $B$  of the whole quantum system under study. Now if we combine an

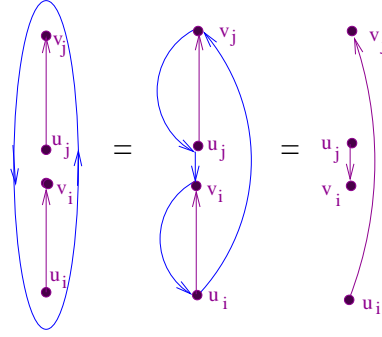


Figure 4: A graphical proof of the identity (3.8).

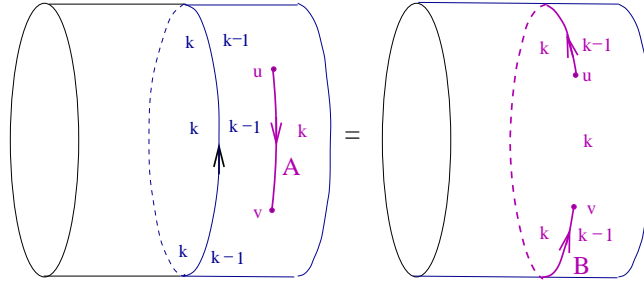


Figure 5: A graphical proof of the equality  $\text{tr } \rho_A^n = \text{tr } \rho_B^n$ .

open cut associated to the cyclic permutation  $k \rightarrow k + 1$  with a closed cut associated with the anti-cyclic permutation  $k \rightarrow k - 1$ , like in Figure 5, the mentioned symmetry evidently interchanges the role of the two subsystems  $A$  and  $B$  and yields at once the fundamental identity

$$\text{tr } \rho_A^n = \text{tr } \rho_B^n, \forall n. \quad (3.9)$$

It is known that this relation, as well as its ensuing consequence (1.2), is valid only if the whole system  $A \cup B$  is in a pure state. This equality is violated at finite temperature because a thermal state is in a mixed state, of course. As a consequence we can infer that the mentioned symmetry should break down at finite  $T$ . For, since the quantum system corresponds to a two-dimensional Euclidean theory with a compactified periodic imaginary time with period  $\beta = 1/T$ , the infinite cylinder reduces to a torus of size  $L \times \beta$ , and the transformation (3.7) is no longer a symmetry of the system, as it transforms  $n$  disjoint tori into a single torus of size  $L \times n\beta$ .

In our numerical experiments we used the vanishing of the difference  $\text{tr } \rho_A^n - \text{tr } \rho_B^n$  as a

sort of thermostat to keep the temperature of the simulated system low enough.

## 4 Entanglement in $Q$ state Potts Models

One of the simplest and more studied models of statistical mechanics is the  $Q$ -state Potts model [16, 17], which is the basic system symmetric under the permutation group of  $Q$  elements. It can be defined by associating with each node  $x$  of an arbitrary lattice  $\Lambda$  the field or spin variable  $\phi_x = 1, 2, \dots, Q$ . Its partition function at the coupling  $J$  is taken to be

$$Z_Q = \sum_{\{\phi\}} e^{-S_Q[\phi]} \quad (4.1)$$

where  $S_Q[\phi] = - \sum_{\langle xy \rangle} J \delta_{\phi_x \phi_y}$  with  $\langle xy \rangle$  ranging over pairs of adjacent nodes on  $\Lambda$ .

In a two-dimensional lattice this system has a typical order-disorder transition which is continuous in the range  $0 \leq Q \leq 4$ . Contrary to the naive expectation, the clusters made of adjacent sites with aligned spins do not play an important role at criticality. A different definition of cluster was proposed [18]. These clusters are defined as adjacent sites with the same spin connected by bonds with probability  $p = 1 - e^{-J}$ . Within such a definition, these clusters behave correctly at the critical point, in the sense that their radius and the density of the percolating cluster scale with the correct critical exponents.

The partition function (4.1) can be rewritten in terms of these clusters using the Fortuin Kasteleyn representation [19]:

$$Z_Q = \sum_{G \subseteq \Lambda} v^{b(G)} Q^{c(G)}, \quad (4.2)$$

where  $v = \frac{p}{1-p} = e^J - 1$ ; the summation is over all spanning subgraphs of  $\Lambda$ , namely the subgraphs made with all the nodes of  $\Lambda$ ;  $b(G)$  is the number of edges of  $G$ , called *active links*, and  $c(G)$  the number of connected components or Fortuin-Kasteleyn (FK) clusters. This formulation of the partition function, sometimes called di-chromatic polynomial, enables one to generalise  $Q$  from positive integers to real and complex values. In particular  $Q = 2$  corresponds to the Ising model and  $Q = 1$  is the random percolation problem.

The implementation of the general method described in Section 3 to evaluate  $\text{tr} \rho_A^n$  is very simple in this case, even if the action in the FK formulation has no longer the form (3.2), as  $c(G)$ , the number of clusters, is a non-local quantity. Each configuration of the  $Q$ -state Potts model is uniquely characterised by the location of the active links. Consider a stack of  $n$  configurations of this kind, defined on a square lattice. Choose an interval  $A$  connecting two arbitrary nodes of the dual lattice and sew together the  $n$  sheets according the rules drawn



in Figure 2 so as to form a covering of the  $n$ -sheeted Riemann surface with a connected square lattice. Note that the sewing operation does not modify the local structure of the lattice nor the location of the active links, while the number of clusters  $c(G)$  may change. Therefore, according to (3.5), we obtain the explicit and simple result

$$\text{tr } \rho_A^n = \langle Q^{c_A - \sum_k c_k} \rangle_n, \quad (4.3)$$

where  $c_k$  denotes the number of clusters of the  $k$ -th replica before sewing and  $c_A$  is the total number of clusters in the stack of  $n$  replicas sewn together along  $A$ ; the vacuum expectation value is taken with respect the system composed of  $n$  decoupled copies of the Potts model under study.

Although so far we have considered for the sake of simplicity a two-dimensional system, it is clear that the formula (4.3) still holds true in any space dimension, provided one defines appropriately the subsystem  $A$ .

A first obvious consequence of (4.3) is that in random percolation, i.e.  $Q = 1$  Potts model,  $\text{tr } \rho_A^n \equiv 1$  for any  $A$  and any  $n$ : as intuitively expected, there is no quantum entanglement in random percolation.

Some further remarks are in order. The  $Q$ -state Potts model on a square lattice for continuous  $Q$  varying between 0 and 4 undergoes a second order phase transition at  $v = \sqrt{Q}$ . Its critical behaviour is described by a CFT with a conformal anomaly  $c$  related to  $Q$  by [20]

$$\sqrt{Q} = 2 \cos \frac{\pi}{m+1} \quad ; \quad c = 1 - \frac{6}{m(m+1)}. \quad (4.4)$$

Random percolation at the percolation threshold corresponds to  $c = 0$ , as the absence of entanglement combined with (2.10) requires.

For  $Q > 1$  there are very efficient non local cluster Monte Carlo algorithms which can be applied for integer  $Q$  [21, 22] as well as for for continuous  $Q$  [23]. They are particularly well suited for accurate estimates of  $\text{tr } \rho_A^n$  through the formula (4.3), as at the heart of these algorithms there is a reconstruction of the FK clusters of the configurations.

We simulated in this way a two-dimensional critical Ising model, which corresponds to a CFT with  $c = \frac{1}{2}$ . We considered very elongated lattices of size  $L \times L'$  with periodic boundary conditions on either side. Typically, the aspect ratios  $L'/L$  were between 4 and 8. This choice amounts to a convenient compromise between (2.10), which is expected to be exactly true only on an infinitely long cylinder, and the numerical experiments, which are necessarily performed on a finite system. As a criterion to decide whether our cylinders were long enough, according with the discussion following (3.9) we compared the values of

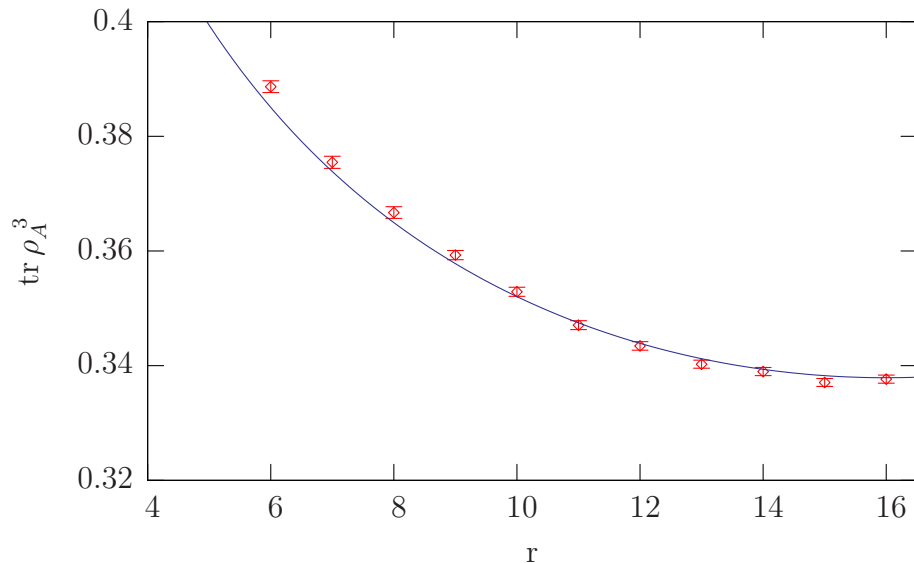


Figure 6: Correlation function of two twist fields in a stack of  $n = 3$  independent copies of a 2D critical Ising model in a square lattice of size  $32 \times 256$ . The data are generated by  $2 \cdot 10^6$  Monte Carlo configurations. The solid line is a one-parameter fit to (2.10).

$\text{tr } \rho_A^n$  and  $\text{tr } \rho_B^n$ , where  $A$  and  $B$  are two complementary cuts along the circumference of the cylinder, as in Figure 5. When  $L'/L = 8$  we found  $\text{tr } \rho_A^n \simeq \text{tr } \rho_B^n$  within the statistical errors. The behaviour of this quantity at  $n = 3$  as a function of the distance of the branch points is depicted in Figure 6. The solid line is a one-parameter fit to (2.10), where the only free parameter is the unknown proportionality constant. We conclude that our numerical experiments reproduce very well the expected conformal behaviour of the Tsallis entropy, even if the actual size of our lattices is not very large.

When considering the entanglement entropy of critical systems corresponding to CFT with negative  $c$ , an intriguing aspect emerges: according to the general expression (1.3),  $S_A$  becomes negative. One is led say that the mixed state obtained by tracing over the degrees of freedom of the complement of  $A$  is in some way more ordered than the vacuum  $|\Psi\rangle$ , which has vanishing entropy. While all that may sound counterintuitive, it has a simple, testable counterpart in the replica approach: according to (2.10), the correlation function of the branch-point twist fields should grow with their distance. One can check it on critical Potts models with  $Q < 1$ , since they correspond to  $c < 0$ . The non-local cluster algorithms [21, 22, 23] are applicable only for  $Q \geq 1$ , however we can resort to a local algorithm [24] which can be implemented in an efficient way in the range  $0 \leq Q \leq 1$  [25, 26].

We performed our numerical experiments at  $Q = 2 - \sqrt{3}$ , whose critical behaviour is

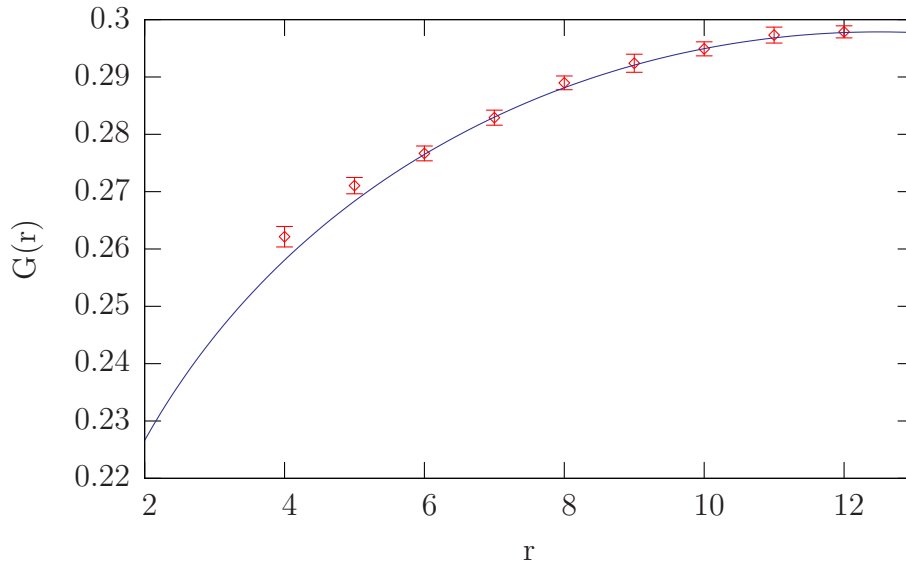


Figure 7: Correlation function of two twist fields in a stack of  $n = 2$  independent copies of a 2D critical  $Q$ -state Potts model, with  $Q = 2 - \sqrt{3}$ , in a square lattice of size  $25 \times 100$ . The corresponding CFT has a negative conformal anomaly ( $c = -\frac{11}{14}$ ). The data come from  $2 \cdot 10^6$  Monte Carlo configurations generated with the algorithm described in [26]. The solid line is a one-parameter fit to (2.10).

described by the (non-unitary) minimal model  $M_{7,12}$ , which has  $c = -\frac{11}{14}$ , according to (4.4). Also in this case we found good agreement with the predicted behaviour of the two-point twist fields correlator, as Figure 7 shows.

One of the most general and fundamental properties of correlation functions of local operators at criticality is the scaling behaviour under a common rescaling of all the dimensional quantities. We may use this principle to test one of the most important findings of the replica approach to entanglement [10], namely the discovery that  $\text{tr} \rho_A^n$  is proportional to a correlation function of twist fields. Although the specific form of  $\text{tr} \rho_A^n$  in the case in which the whole system is enclosed in a square box of side  $L$  and the subsystem  $A$  consists of  $N$  disjoint intervals  $A \equiv (u_1, v_1), \dots, (u_N, v_N)$  is not actually known, (1.6) implies the following homogeneity property (see Figure 8)

$$\text{tr} \rho^n(\lambda u_1, \lambda v_1, \dots, \lambda u_N, \lambda v_N, \lambda L) = \lambda^{-4n\Delta_n N} \text{tr} \rho^n(u_1, v_1, \dots, u_N, v_N, L), \quad (4.5)$$

where  $\lambda$  is any positive rescaling factor and  $\Delta_n$  is the scaling dimension (1.5) of the  $2N$  branch point twist fields. We checked this formula in critical Ising systems in the cases  $N = 1$  and  $N = 2$ , finding perfect agreement for boxes large enough, as Figure 8 shows:

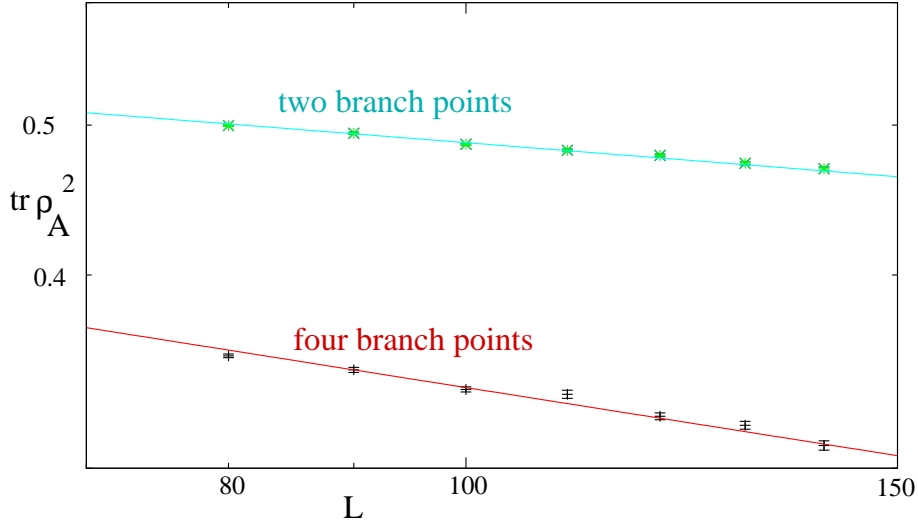


Figure 8: Comparison of the scaling behaviour of the twist correlator in the case of two and four branch points. The  $x$  axis is in a log scale and the numerical data lie on straight lines as expected. According to (4.5) the slope is exactly  $4n\Delta_n N$ , where  $2N$  is the number of branch points, while the intercept is the only fitting parameter. In this instance the critical model is the Ising model and  $n = 2$ , therefore  $4n\Delta_n = \frac{1}{8}$ .

the slopes of the two straight lines match precisely with the predicted value  $4n\Delta_n N$ . We checked in the same way the scaling properties of the three-point function (2.16) proposed in the present paper, which corresponds to put  $N = \frac{3}{2}$  in the above formula, finding again a good agreement (see Figure 9), even if such a case is more demanding from a computational point of view.

We also performed a numerical experiment to settle whether in the limit  $|u_1 - u_2| \rightarrow 0$  the observable  $\text{tr} \rho_{A=\{(u_1, v_1)(u_2, v_2)\}}^n$  vanishes, as predicted by (1.7), or diverges, as argued in Section 2. For this purpose we considered two collinear intervals, as sketched in Figure 10, on a stack of 3 replicas. In order to reduce the noise, instead of considering as in the other numerical experiments three independent Ising systems, we simulated the model on a three-sheeted Riemann surface  $\mathcal{R}_3$  with a cut in  $(u_1, v_1)$ , thus the measured observable was

$$\langle \Phi_3^-(u_1) \Phi_3^+(v_1) \Phi_3^-(u_2) \Phi_3^+(v_2) \rangle_{\mathcal{R}_3} \equiv \frac{\langle \Phi_3^-(u_1) \Phi_3^+(v_1) \Phi_3^-(u_2) \Phi_3^+(v_2) \rangle_3}{\langle \Phi_3^-(u_1) \Phi_3^+(v_1) \rangle_3}. \quad (4.6)$$

Figure 10 shows that this quantity grows as  $|u_1 - u_2|$  decreases, even if within this set up it is not possible to accurately measure the associated exponent, which according to (2.13) should be exactly half that of a pair of branch points of opposite charge.

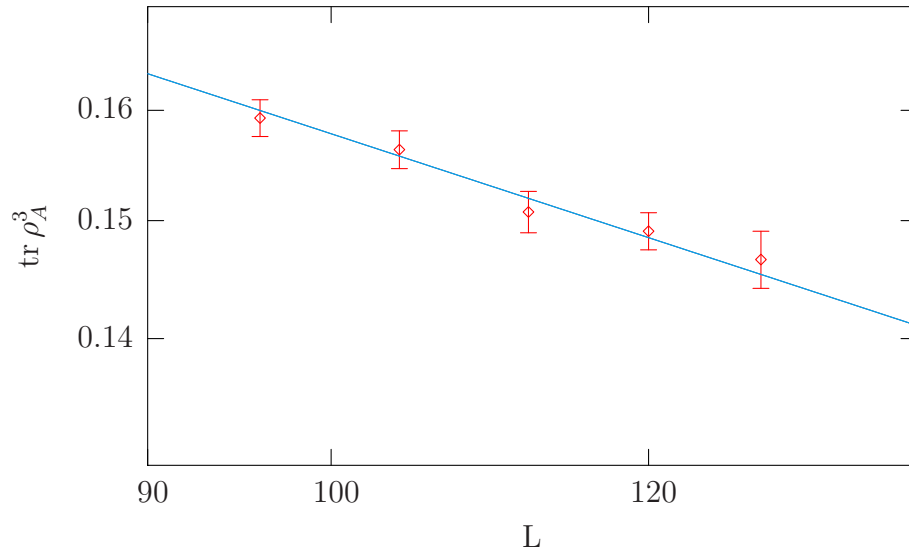


Figure 9: Scaling behaviour of the twist correlator in the case of three branch points of a critical Ising model defined on a stack of  $n = 3$  replicas in the configuration depicted in Fig.1. The  $x$  axis is in a log scale and the numerical data lie on a straight line as expected. The slope of the solid line is exactly  $6n\Delta_n = \frac{1}{3}$  as predicted by (2.16). The data of larger lattices are generated by  $\sim 10^7$  Monte Carlo configurations.

## 5 Conclusions

In this paper we discussed both analytically as well as numerically some properties of the trace of the  $n$ -th power of the reduced density matrix  $\rho_A$  in the special case in which  $A$  is a subsystem of a quantum system described by a conformal field theory in two dimensions. From the analytical point of view we pointed out that when  $A$  is composed with more than a single interval the explicit formulae proposed in [10] suffer from some inconsistencies. The origin of these can be traced to the fact that in the derivation of the general formulae certain singularities of the Schwarzian derivative have been overlooked. Of course a moot derivation does not imply a wrong final result, thus it is well possible that the formulae for the entanglement entropy obtained by analytic continuation to  $n \rightarrow 1$  are still correct.

From the computational point of view we developed a simple method which allows us to directly evaluate  $\text{tr } \rho_A^n$  as a vacuum expectation value. We applied it to two different critical systems in two-dimensional Euclidean lattices, corresponding to two different values of conformal anomaly  $c$ , finding perfect agreement with the predicted formulae in the case in which  $A$  is composed by a single interval in a system of finite size [10].

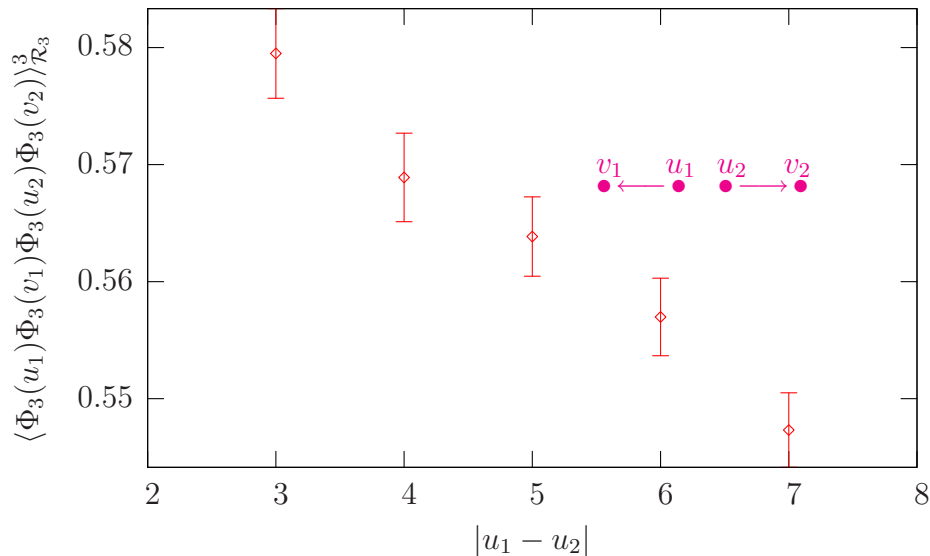


Figure 10: In a critical Ising model defined on a stack of  $n = 3$  replicas, the subsystem  $A$  is chosen to consist of two collinear segments  $(u_1, v_1)$   $(u_2, v_2)$  as indicated in Figure and the quantity (4.6) is plotted versus  $|u_1 - u_2|$ . The size of the lattice is  $128 \times 128$  and  $|u_1 - v_1| = |u_2 - v_2| = 32$ . The data are generated by  $2 \cdot 10^6$  Monte Carlo configurations.

A distinguishing feature of the present method is that the simulations are performed in the unperturbed system: the  $n$  replicas of the system under study do not interact with each other nor are sewn together along some particular subsystem  $A$ . The information on entanglement is encoded in the observable  $\mathbb{O}$  whose evaluation does not perturb the system. An obvious advantage of such an approach is that one can exploit the same set of configurations to obtain information on the entanglement entropy for a variety of subsystems.

We would also like to remark that the usual method to measure  $c$  in lattice simulations is very different from that one may infer from the present paper. The standard method originates from the observation that the first subleading correction to the free energy of a CFT on a long cylinder is universal and proportional to  $c$  [14], however the free energy cannot be directly measured in lattice simulations, thus usually one circumvents this difficulty by measuring and integrating the internal energy, with an inevitable loss of precision. The method described in this paper may be viewed as a novel and powerful tool to directly measure  $c$ : the rescaling property (4.5) of the Tsallis entropy tells us that a measurement of  $\text{tr} \rho_A^n$  in two lattices of different size suffice to fix the slope of the upper straight line drawn in Figure 8, and hence the value of  $c$ .

To conclude, notice that the proposed numerical method can also easily be applied to

critical and non-critical systems in any space-time dimensions. For instance, adding one more dimension to the Ising system simulated in this paper and applying Kramers and Wannier duality [27], one may obtain information on the entanglement entropy of a confining gauge theory, an issue of growing interest in the last years [28, 29, 30, 31].

## 6 Acknowledgements

FG thanks the Galileo Galilei Institute for Theoretical Physics for hospitality and the INFN for partial support during the initial phase of this work. We also wish to thank R. Tateo for extensive, helpful discussions, P. Calabrese and J. Cardy for fruitful, stimulating correspondence.

## References

- [1] G. 't Hooft, “On The Quantum Structure Of A Black Hole,” Nucl. Phys. B **256** (1985) 727; L. Bombelli, R. K. Koul, J. H. Lee and R. D. Sorkin, “A Quantum Source Of Entropy For Black Holes,” Phys. Rev. **D34** (1986) 373.
- [2] M. Srednicki, “Entropy and area,” Phys. Rev. Lett. **71**(1993) 666 [arXiv:hep-th/9303048].
- [3] C. G . Callan and F. Wilczek, “On Geometric Entropy,” Phys. Lett. B **333**(1994) 55 ; [arXiv:hep-th/9401072]. J. S. Dowker, “Remarks On Geometric Entropy,” Class. Quant. Grav. **11** (1994) L55; [arXiv:hep-th/9401159]; D. Kabat and M. J. Strassler, “A Comment on entropy and area,” Phys. Lett. B **329** (1994) 46 [arXiv:hep-th/9401125]; D. Kabat, “Black hole entropy and entropy of entanglement,” Nucl. Phys. B **453**(1995) 281 [arXiv:hep-th/9503016]; D.V.Fursaev, S.N.Solodukhin “On the Description of the Riemannian Geometry in the Presence of Conical Defects” Phys.Rev. D **52** (1995) 2133 [arXiv:hep-th/9501127].
- [4] H. Casini, “Geometric entropy, area, and strong subadditivity,” Class. Quant. Grav. **21** (2004) 2351 [arXiv:hep-th/0312238].
- [5] S. Ryu and T. Takayanagi, “Holographic derivation of entanglement entropy from AdS/CFT,” Phys. Rev. Lett. **96** (2006) 181602 [arXiv:hep-th/0603001]; S. Ryu and T. Takayanagi, “Aspects of holographic entanglement entropy,” JHEP **0608** (2006) 045 [arXiv:hep-th/0605073].

- [6] R. Emparan, “Black hole entropy as entanglement entropy: A holographic derivation,” JHEP **0606** (2006) 012 [arXiv:hep-th/0603081]; D. V. Fursaev, “Proof of the holographic formula for entanglement entropy,” JHEP **0609** (2006) 018 [arXiv:hep-th/0606184]; S. N. Solodukhin, “Entanglement entropy of black holes and AdS/CFT correspondence,” Phys. Rev. Lett. **97** (2006) 201601 [arXiv:hep-th/0606205].
- [7] C. Holzhey, F. Larsen, F. Wilczek “Geometric and Renormalized Entropy in Conformal Field Theory” Nucl.Phys. B**424** (1994) 443 [arXiv:hep-th/9403108]
- [8] G. Vidal, J. I. Latorre, E. Rico, A. Kitaev, “Entanglement in quantum critical phenomena”, Phys. Rev. Lett. **90**, (2003) 227902 [arXiv:quant-ph/0211074]; J. I. Latorre, E. Rico, G. Vidal, “Ground state entanglement in quantum spin chains”, Quant. Inf. and Comp. **4** (2004) 48 [arXiv:quant-ph/0304098].
- [9] H. Casini, M. Huerta, “A finite entanglement entropy and the c-theorem” Phys.Lett. B **600** (2004) 142 [arXiv:hep-th/0405111].
- [10] P. Calabrese, J. Cardy “Entanglement Entropy and Quantum Field Theory” J.Stat.Mech. **0406** (2004) P002 [arXiv:hep-th/0405152].
- [11] M. -C. Chung and I. Peschel, “Density-matrix spectra for two-dimensional quantum systems” Phys. Rev. B **62** (2000) 4191; M. Cramer, J. Eisert and M. B. Plenio, “Statistics dependence of the entanglement entropy,” Phys. Rev. Lett. **98** (2007) 220603 [arXiv:quant-ph/0611264].
- [12] C. Tsallis “Possible generalization of Boltzmann-Gibbs statistics”, J. Stat. Phys.**52** (1988) 479.
- [13] J.L. Cardy, O.A. Castro-Alvaredo, B. Doyon, “Form factors of branch-point twist fields in quantum integrable models and entanglement entropy”, J. Stat. Phys. **130** (2007) 129 [arXiv:0706.3384 [hep-th]]; B. Doyon, “Bi-partite entanglement entropy in massive two-dimensional quantum field theory,” arXiv:0803.1999 [hep-th].
- [14] I. Affleck, “Universal Term In The Free Energy At A Critical Point And The Conformal Anomaly,” Phys. Rev. Lett. **56** (1986) 746; H. W. J. Blöte, J. L. Cardy, M. P. Nightingale, “Conformal Invariance, the Central Charge, and Universal Finite Size Amplitudes at Criticality,” Phys. Rev. Lett. **56**(1986) 742.



- [15] E.L. Ince, “Ordinary Differential Equations”, Dover Publications, Inc., New York, 1956.
- [16] R.B. Potts, “Some generalized order - disorder transformations,” Proc. Camb. Phil. Soc. **48** (1952) 106.
- [17] F.Y. Wu, “The Potts model”, Rev. Mod. Phys. **54** (1982) 235.
- [18] A. Coniglio and W. Klein, “Clusters and Ising critical droplets: a renormalization group approach” J. Phys. A **13** (1980) 2775; A. Coniglio and F. Peruggi, “Cluster and droplets in the q-state Potts model,” J. Phys. A **15** (1982) 1873.
- [19] C.M. Fortuin and P.W. Kasteleyn, “On the Random cluster model. 1. Introduction and relation to other models,” Physica **57** (1972) 536.
- [20] B. Nienhuis, “Critical behavior of two-dimensional spin models and charge asymmetry in the Coulomb gas”, J. Statist. Phys. **34** (1984) 731; P. di Francesco, H. Saleur and J. B. Zuber, “Relations Between The Coulomb Gas Picture And Conformal Invariance Of Two-Dimensional Critical Models”, J. Statist. Phys. **49** (1987) 57.
- [21] R.H. Swendsen and J.-S. Wang, “Nonuniversal Critical Dynamics in Monte Carlo Simulations”, Phys. Rev. Lett. **58** (1987) 86.
- [22] U. Wolff, “Collective Monte Carlo Updating for Spin Systems,” Phys. Rev. Lett. **62** (1989) 361.
- [23] L.Chayes and J. Machta, “Graphical representations and cluster algorithms II”, Physica A **254** (1998) 477.
- [24] F. Gliozzi, “Simulation of Potts models with real q and no critical slowing down,” Phys. Rev. E **66** (2002) 016115 [arXiv:cond-mat/0201285].
- [25] Y. Deng, H. W.J. Blöte and B. Nienhuis, “Backbone exponents of two-dimensional q-state Potts model: A Monte Carlo investigation” Phys. Rev. E **69** (2004) 026114.
- [26] F. Gliozzi, “Confining vacua and Q-state Potts models with  $Q < 1$ ,” PoS **LAT2007** (2007) 304 [arXiv:0708.4332 [hep-lat]].
- [27] H. A. Kramers and G. H. Wannier, “Statistics of the two-dimensional ferromagnet. Part 1,” Phys. Rev. **60** (1941) 252.

- [28] T. Nishioka and T. Takayanagi, “AdS bubbles, entropy and closed string tachyons,” JHEP **0701** (2007) 090 [arXiv:hep-th/0611035].
- [29] I. R. Klebanov, D. Kutasov and A. Murugan, “Entanglement as a Probe of Confinement,” Nucl. Phys. B **796** (2008) 274 [arXiv:0709.2140 [hep-th]].
- [30] A. Velytsky, “Entanglement entropy in d+1 SU(N) gauge theory,” Phys. Rev. D **77** (2008) 085021 [arXiv:0801.4111 [hep-th]].
- [31] P. V. Buividovich and M. I. Polikarpov, “Numerical study of entanglement entropy in SU(2) lattice gauge theory,” Nucl. Phys. B **802** (2008) 458 [arXiv:0802.4247 [hep-lat]]; P. V. Buividovich and M. I. Polikarpov, “Entanglement entropy in gauge theories and the holographic principle for electric strings,” arXiv:0806.3376 [hep-th].